Strontium Titanate (SrTiO₃) for Adsorption of Cd(II) Ions and Photodegradation of Methylene Blue Dye in Aqueous Solutions

Amanda das Graças Barbosa* [ID] [a], Vanessa Nunes Alves [ID] [a], Cristiano Morita Barrado [ID] [a], Tânia Regina Giraldi [ID] [b], Fabiana Villela Motta [ID] [c], Benjamim Monteiro da Silva Neto [c], and Alberthmeiry Teixeira de Figueiredo [ID] [a]

Strontium titanate (SrTiO₃ – STO) is a metal oxide with a perovskite structure that has attracted scientific interest due to its various applications. The present study aims to synthesize STO and evaluate its potential for adsorption of Cd(II) ions and photodegradation of methylene blue. The STO samples were synthesized using the polymer precursor method and microwave-assisted hydrothermal method. X-ray diffraction analysis confirmed the formation of STO crystalline phase, and scanning electron microscopy revealed differences morphology to distinct synthesis method used. STOMW sample was able to remove 94.7% of Cd(II) ions in solution, while STOPP sample demonstrated good photocatalytic activity, with 80% dye degradation. The results indicate that STO is a promising material for the removal of both inorganic and organic contaminants from aqueous waste.

Graphical abstract
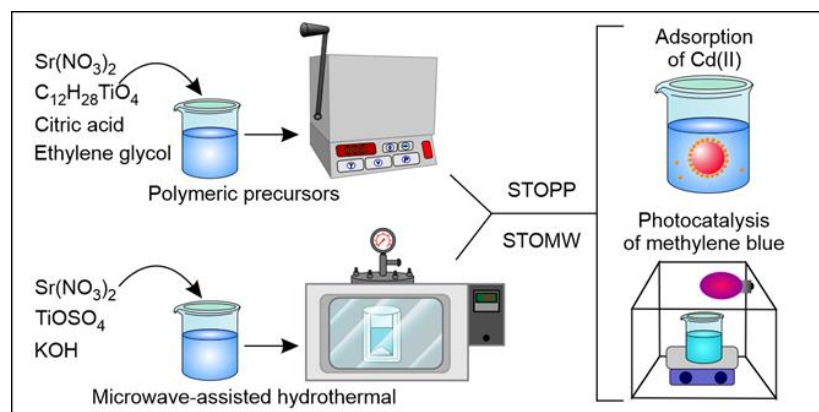
1. Introduction

Adsorption is a powerful method for removing metal ions from wastewater, with nanomaterials like oxides showing significant potential due to their unique properties and performance. This potential stems from their significantly larger surface areas, enabling faster and more efficient adsorption of metals from wastewater compared to conventional materials, making them economical and environmentally friendly solutions for water treatment [1,2].

[a] Institute of Chemistry, Federal University of Catalãol (UFCAT). Av. Dr. Lamartine Pinto de Avelar, 1120 Vila Chaud, zip code 75704-020, Catalão, Goiás, Brazil. [b] Institute of Science and Technology, Federal University of Alfenas (Unifal), Campus Poços de Caldas. Rodovia José Aurélio Viela (BR 267 Km 533), 11.999 - Cidade Universitparia. Poços de Caldas-MG. [c] LSQM – Laboratory of Chemical Synthesis of Materials – Department of Materials Engineering, Federal University of Rio Grande do Norte – UFRN, P.O. Box 1524, Natal RN, Brazil. *Corresponding author: E-mail: **amandadasgracas60@gmail.com**

In particular, SrTiO$_3$ (STO) is a metal oxide with a cubic perovskite structure, synthesized via multiple methods. It has attracted much attention as an efficient material for different applications such as degradation of organic dyes and good adsorption capacity for metal ions [3-5]. There are many studies reporting the use of STO for removing metallic ions from wastewater. In addition, there is a consensus in these studies that the surface area of nanocrystalline STO is responsible for the observed adsorption capacity. Similarly, STO nanoparticles exhibit high photocatalytic activity toward dyes. It has a wide bandgap, typically around 3.2 eV, allowing the absorption of UV light, which is ideal for exciting electrons from the valence band to the conduction band [6].

The parameters affecting metal ion removal efficiency include pH, temperature, initial adsorbate concentration, and initial metallic ion concentration. These factors significantly influence the removal efficiency for treating wastewater [2,7]. In addition, it is desirable that the adsorbents can be used many times without losing their adsorption capacity [2,7].

In this work, SrTiO$_3$ particles were synthesized by two different synthesis methods. The main objective of this work is to evaluate the STO ability to remove cadmium ions from an aqueous medium, and degradation of methylene blue dye. Three results can be highlighted here: (i) obtaining of STO at room temperature without any heat treatment, (ii) fast removal of all toxic cadmium ions, and (iii) good dye degradation capacity. The characteristics of STO particles are discussed in detail based on the X-ray diffraction (XRD) and scanning electron microscopy (SEM). The adsorption properties were analyzed to identify the removal of Cd^{2+} ions in aqueous media, and it was evaluated the effect of the adsorption pH of cadmium ions by STO samples.

2. Material and Methods

SrTiO$_3$ (STO) samples was sinthesized by two distincts methods: (i) HTMW processing (STOMW sample), and the polymeric precursor method (STOPP sample).

In the HTMW processing, the SrTiO$_3$ (STO) samples were synthesized using the following precursors: TiO(SO$_4$) (Sigma-Aldrich, ≥ 98%), Sr(NO$_3$)$_2$ (Synth, 99%) and KOH (Synth, 85%). These reagents were used without further purification. In the experimental procedure, 0.01 mol of titanium precursor and strontium precursor were dissolved separately in distilled water. The two solutions were then mixed and 50 mL of KOH (6.0 mol.L^{-1}) was added. To produce the remaining STO samples, the Standard Suspension was transferred to a Teflon vessel and inserted into a reactor, which was sealed and placed in a hydrothermal-microwave (HTMW) system, where it was kept at 140 ^{o}C for 4 minutes. The HTMW system was operated at a frequency of 60 Hz and with a maximum power of 1500 W, under pressure of approximately 3 bar. After processing, the reactor was cooled to room temperature and the resulting precipitate was washed repeatedly in distilled water and dried at 80 ^{o}C for 12 hours.

In the polymeric precursor method, MPP method, titanium citrates were formed by the dissolution of titanium-(IV) isopropoxide in an aqueous solution of citric acid (60-70 °C). After homogenization of the Ti solution, Sr(NO$_3$)$_2$ was slowly added. After the complete dissolution of the Sr(NO$_3$)$_2$ salt, ethylene glycol was added to polymerize the mixed citrates by a polyesterification reaction. The molar ratio of strontium to titanium was 1:1 and the ratio of citric acid to ethylene glycol was set at 60:40 mass ratio. The polymeric resin was pyrolized at 300 °C for 2 h, resulting in a powder containing organic residues due to the method employed. The obtained powder was deagglomerated, and then it was heat treated at 600 °C for 2 h.

To determine their structural characteristics, the powders were characterized by X-ray powder diffraction (XRD) in a Shimadzu XRD 6100 diffractometer, using CuKα (k = 1.5406 Å) radiation. The data were collected in fixed-time mode, from 20° to 80° in the 2θ range, using a divergence slit of 0.5^o and receiving slit of 0.3 mm and a step size of 0.02^o. Microstructural and morphological analyses were performed by field emission scanning electron microscopy (FESEM, Zeiss Supra 35), using 2 to 4 kV under different levels of magnification.

Information about the functional groups present in the materials was obtained through characterization by infrared spectroscopy, using a Perkin Elmer spectrophotometer, model FTIR Frontier Single Range – MIR, with scanning in the range of 4000 to 270 cm^{-1} and a resolution of 1 cm^{-1}.

In addition, the surface charge of the particles was also estimated as a function of the pH of the solution in which they are immersed. The characterization of the pH at the point of zero charge (pH$_{pzc}$) is useful in adsorption studies and involves adding 2 mg of the STO to 5 mL of aqueous solutions with pH ranging from 1 to 12. After 24 hours of resting at room temperature, the final pH of the solution was measured.

The adsorption capacity of the synthesized particles was investigated for Cd(II) ions. For this study, Cd(II) solutions at 1.5 mg L^{-1} were prepared at different pH values (1, 7, and 9), adjusted with the addition of NaOH 0.1 mol L^{-1} and/or HNO$_3$ 0.1 mol L^{-1}. 2 mg of the adsorbent were added to 5 mL of these solutions, followed by stirring at 270 rpm for 30 minutes. After the contact time, the adsorbent was removed by centrifugation, and the supernatant was analyzed by flame atomic absorption spectroscopy (FAAS) to determine the remaining Cd(II) concentration in the solution after the adsorption process. All the experiments were performed in triplicate.

Cadmium ions were quantified in a Varian SpectrAA 220 flame atomic absorption spectrometer (Victoria, Australia) equipped with a cadmium hollow cathode lamp and a deuterium lamp for background correction. The FAAS instrument was operated as recommended by the manufacturer: lamp current of 4 mA, wavelength of 228.8 nm, slit width of 0.1 nm, burner height of 17 mm, acetylene flow rate of 2.0 L min^{-1}, and airflow rate of 13.5 L min^{-1}.

To evaluate the photocatalytic activity of the synthesized materials, four tests were conducted: 1) adsorption of methylene blue (MB) dye on the surface of STO, 2) degradation of the dye under sunlight, 3) degradation of MB in a UV box, and 4) determination of the bandgap of the STO samples through reflectance measurement. In tests 1 to 3, an initial MB concentration of 5 mg L^{-1} was used, with the final concentration measured by UV-Vis spectroscopy on a Shimadzu spectrophotometer (UV-2600 model).

The photocatalytic activity of the samples under sunlight was carried out for a period of 100 minutes, with an average solar power of 789 W/m² throughout the experiment, ranging from a maximum of 880 W/m² to a minimum of 678 W/m².

The dye degradation under UV light was performed using 6 UV lamps, each with a power of 18 W (Philips TUV, 254 nm = 4.9 eV) for 100 minutes. In these experiments, the adsorption time was fixed at 40 minutes, and degradation aliquots were taken and analyzed every 20 minutes.

3. Results and Discussion

The STO was successfully obtained. The Figure 1 shows the diffractograms of the synthesized samples. Comparison with the ICDD crystallographic card No. 00-005-0634 indicates that the samples exhibit diffraction patterns corresponding to the crystalline phase of $SrTiO_3$, with a lattice parameter of a = 3.9051 Å and space group Pm-3m (221). Therefore, both synthesis methods used were effective in obtaining the desired oxide, without the formation of secondary phases.
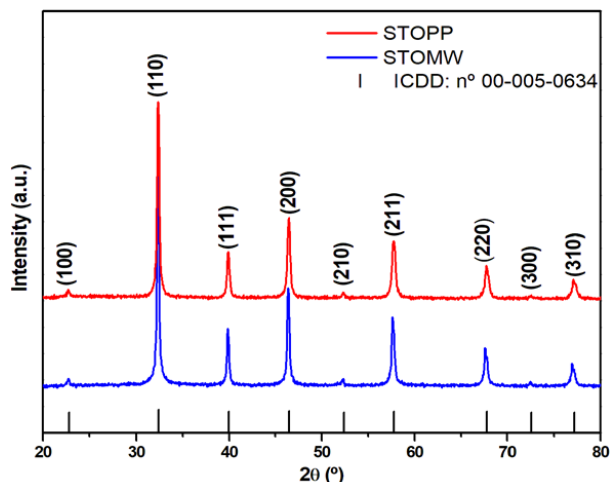
Regarding the STOW sample, XRD analysis was performed on the material before and after the HTMW processing. As shown in Figure 2, the crystalline phase of STO is obtained even without microwave interference. This condition is promising as it makes the process more reproducible, reduces energy consumption, and requires less synthesis time. However, the heating provided by the microwaves increases the crystallinity of the material, as the STOMW sample shows more intense diffraction peaks.
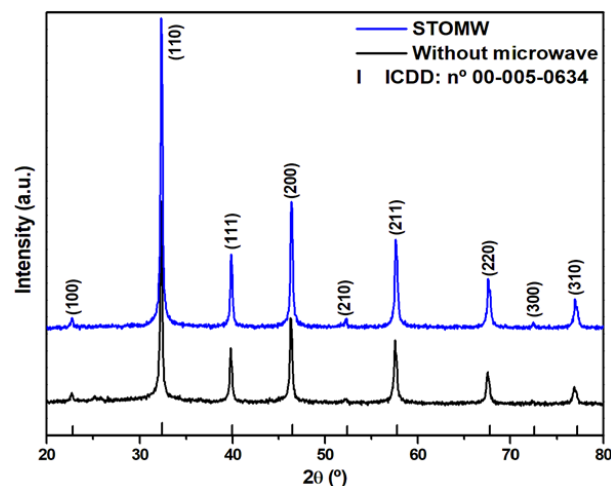

Fig. 1. Diffractograms of the obtained STO samples.

Fig. 2. Diffractograms of the STOMW sample with and without HTMW processing.

The average crystallite size of the samples was calculated using the Scherrer method, which considers the full width at half maximum of the most intense peak in the diffractogram. The STOPP and STOMW samples showed average crystallite sizes of 35 and 42 nm, respectively.

The FE-SEM micrographs (Fig. 3) confirm that the morphology of the STO particles is directly influenced by the synthesis route. The MPP method yielded particles in the form of irregular block-shaped structures with a rigid appearance, while the HTMW method produced smaller particles with an almost cubic shape.
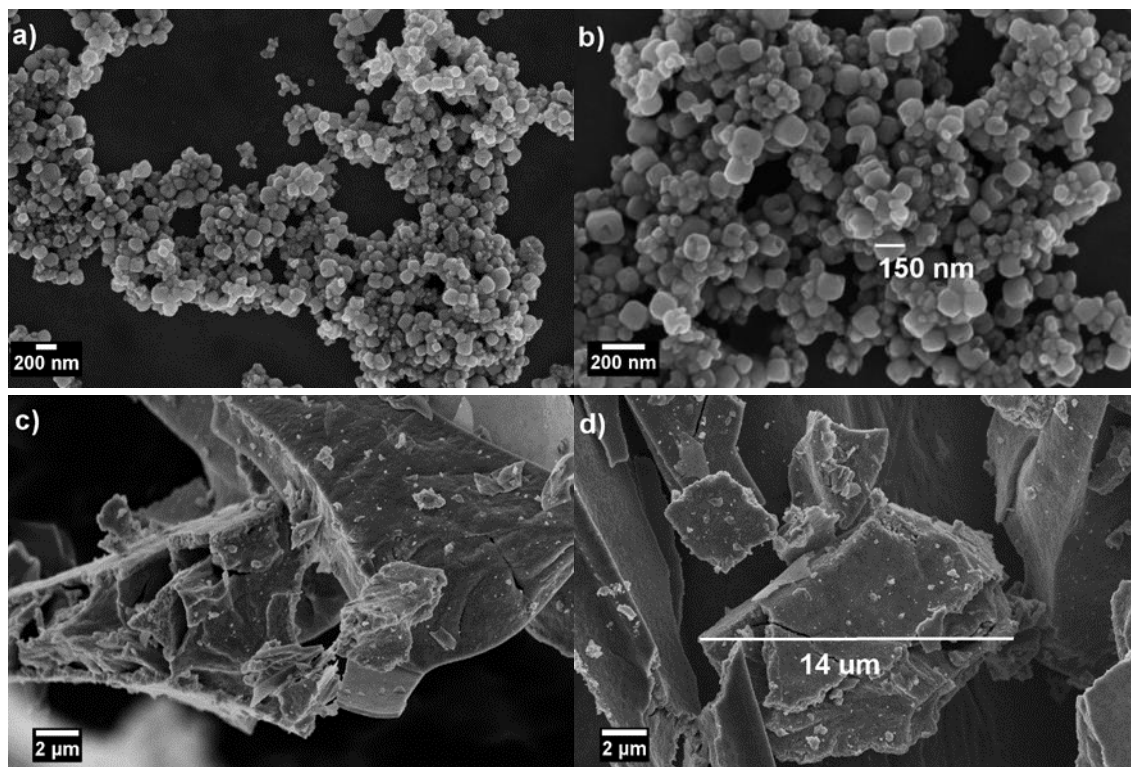

Fig. 3. FE-SEM micrographs of the samples: STOMW (a,b), and STOPP (c,d).

The morphology observed in STOPP sample is the result of an intrinsic characteristic of the synthesis method, where the high thermal energy used to remove organic matter provokes the sintering of the nanoparticles, causing the nanometric monocrystals to aggregate into larger particles [8-10].

The infrared spectroscopy characterization was used to identify the functional groups present in the material, which will interact with the adsorbate and promote the adsorption process. As shown in Figure 4, bands were identified at approximately 3430, 1748, 1459, 1370, 1225, 860, 537, and 437 cm^{-1} in both STO samples.
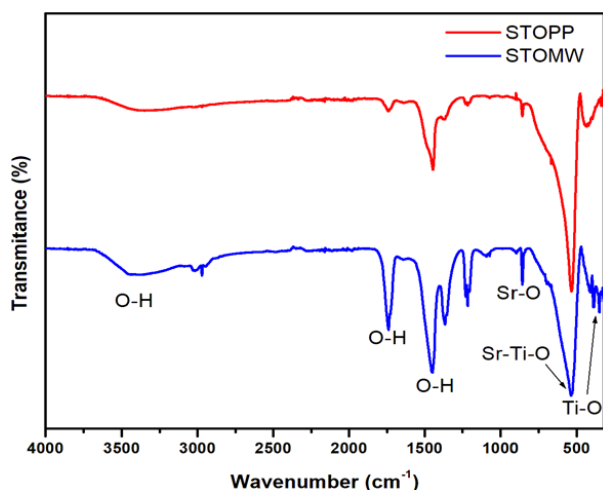

Fig. 4. FT-IR spectra of the obtained STO samples.

The bands observed around 3430, 1742, and 1452 cm^{-1} are associated with the presence of OH groups [11-14]. For the STOPP sample, these bands show lower intensity, indicating a reduced amount of these groups on the surface of the material, possibly due to the high-temperature thermal treatment used in the MPP method.

The bands at 860 and 437 cm^{-1} are attributed to the stretching of the $Ti-O_6$ octahedron and the Ti-O bending vibration, respectively [14,15]. The intense band at ~537 cm^{-1} is characteristic of STO and corresponds to the vibration of the Sr-Ti-O bond [15,16].

Another essential characterization in adsorption processes is the study of the pH at the point of zero charge (pH_{PZC}), which corresponds to the pH at which the surface charge of the adsorbent is zero [17]. In this context, if $pH_{solution}$ < pH_{PZC}, the STO will exhibit a positive surface charge due to the protonation of the OH groups present on its surface. On the other hand, if $pH_{solution}$ > pH_{PZC}, it will be negatively charged due to the deprotonation of the OH groups [17,18].

Based on the graph in Figure 5, the determined pH_{PZC} values are 8.3 and 7.5 for STOPP and STOMW samples, respectively. This difference is possibly related to the lower amount of OH groups present on the surface of STOPP sample, as evidenced by the FT-IR spectra.

The choice of solution pH is essential to optimize the adsorption process, since this parameter affects the surface charge of the adsorbent and the distribution of metallic ion species. The adsorption studies of Cd(II) ions on the STO surface were conducted at pH values of 1, 7, and 9, where the metal ion is present in the form of cations [19].

It is observed that adsorption is not favored at acidic pH for both samples (Fig. 6). On the other hand, the removal of

Cd(II) ions at pH 7 and 9 ranges from 70% to 95%. Theoretically, the adsorption process would not be favored at pH 7, as both the STO and the metal ions are positively charged under these conditions. The effective removal observed at this pH suggests that the adsorption of Cd(II) ions on the STO surface does not occur solely through electrostatic interactions. The adsorption of metallic ions on oxide surfaces can occur due to other types of interactions, such as ion exchange, complexation, hydrogen bonding, and Van der Waals forces [20].
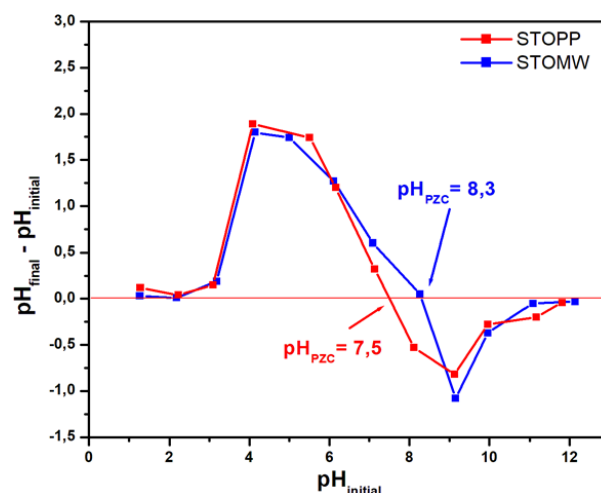

Fig. 5. pH at the point of zero charge (pH_{PZC}) of the STO samples.
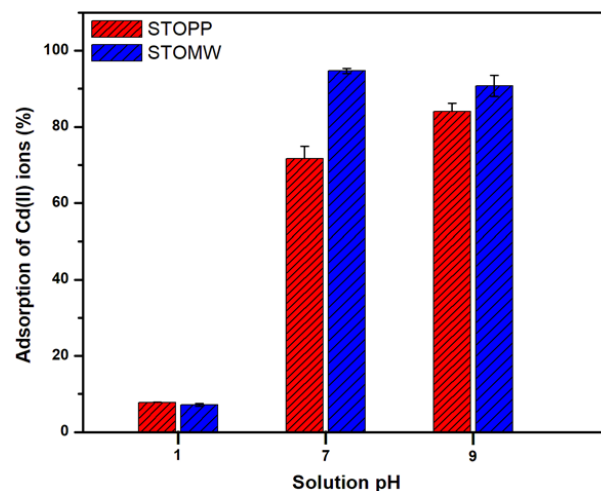

Fig. 6. Adsorption of Cd(II) ions on the surface of STO samples.

The STOMW sample in pH 7 solution stands out, achieving the removal of 94.7% of the ions. As a result, the solution that initially contained 1,5 mg L^{-1} of Cd(II) ions now contains only about 0,08 mg L^{-1}. The superior adsorption capacity of STOMW sample is likely attributed to the higher number of available OH functional groups on this material.

Therefore, the HTMW processing proves to be a promising synthesis method for enhancing the adsorption capacity of the oxide. Other advantages of using microwaves include homogeneous volumetric heating of the reaction medium, energy savings, and reduced synthesis time [21,22].

The adsorption capacity of STO was also tested against methylene blue (MB) dye, varying the contact time from 5 to 60 minutes (Fig. 7). During the studied period, the maximum

removal was 10% for STOMW and 6.7% for STOPP samples. So, it can be concluded that the removal of MB from aqueous solution using STO is not effective through the adsorption process, and an adsorption time of 40 minutes was set. After this contact time, the MB solutions were exposed to UV radiation or sunlight to assess the dye degradation through the photocatalysis process.
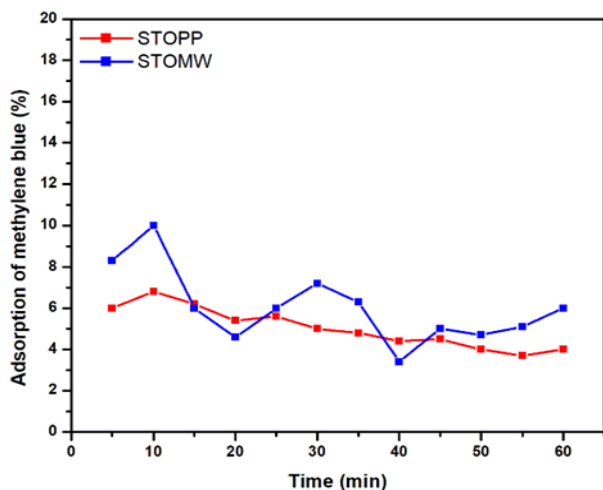

Fig. 7. Adsorption of methylene blue (MB) on the STO surface.

It can be observed that the dye degradation is more intense under sunlight than under UV radiation (Fig. 8). After 100 minutes of exposure to sunlight, the STOPP and STOMW samples degraded 54% and 80% of the dye, respectively. Under UV radiation, degradation was 28% for STOMW and 21% for STOPP samples.

The better photocatalytic performance under sunlight may be related to the high rate of incident energy and the material's greater ability to absorb this type of energy [23]. It is worth noting that the high intensity of solar light also helps reduce the recombination process of e^-/h^+ pairs, thereby enhancing the generation of radicals responsible for dye degradation [23].

In the photocatalysis process, STOPP sample proved to be more efficient and promising, unlike what was observed in the adsorption of Cd(II) ions. This fact can be attributed to the lower bandgap value calculated for this sample, 3.42 eV, compared to the 3.57 eV bandgap of STOMW sample [6].

The studies on the adsorption capacity of STO and its photocatalytic activity confirmed that this material is promising for the removal of Cd(II) ions and MB from aqueous solutions. The studies showed that the particle synthesis method directly influences its application. While STOMW sample proved effective for Cd(II) ion removal, with 95% removal, STOPP sample stood out in the degradation of methylene blue dye, achieving 80% degradation under sunlight.

4. Conclusions

STO was efficiently obtained both by the polymer precursor method and by microwave-assisted hydrothermal synthesis. The diffractograms confirmed the synthesis of pure and crystalline materials, with crystallite sizes in the nanometer range. The synthesis method directly influenced the morphology and functional groups present in the samples.

STOMW sample demonstrated significant potential for the removal of Cd(II) ions from aqueous solutions, being capable of removing 94.7% of these ions in a neutral pH solution. Meanwhile, STOPP sample showed promising photocatalytic activity under sunlight, achieving 80% methylene blue degradation.

These studies highlight the importance of $SrTiO_3$ as a promising material for wastewater treatment applications, contributing to the mitigation of pollution from metal ions and dyes.
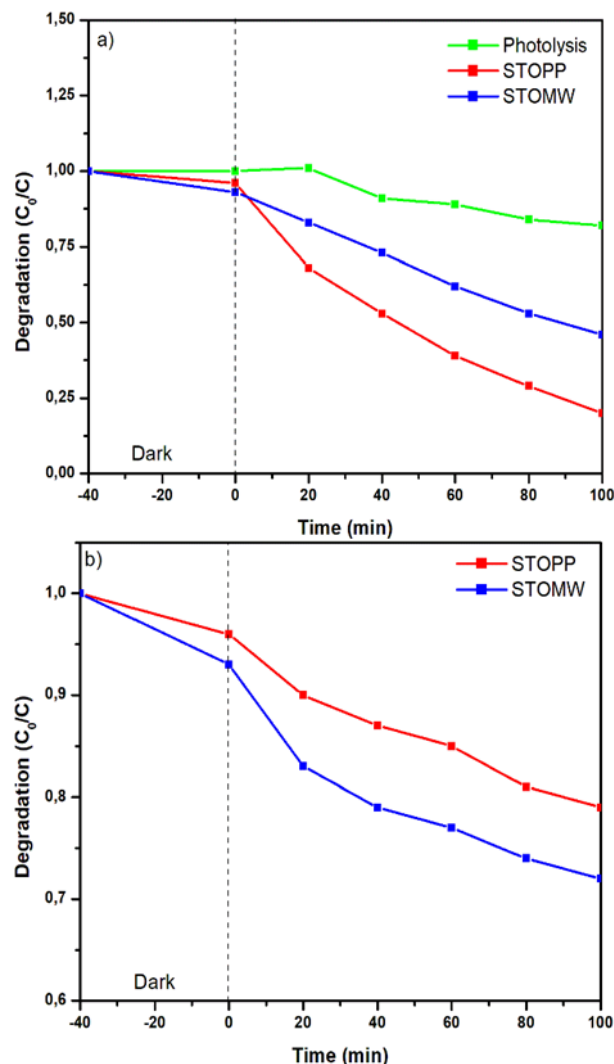

Fig. 8. Photocatalytic activity in MB solution of the STO samples under radiation: a) Solar and b) UV.

References and Notes

[1]   Singh, N. B.; Nagpal, G.; Agrawal, S.; Rachna. *Environ. Technol. Innovation*. **2018**, *11*, 187. **[Crossref]**

[2]   Sadegh, H.; Ali, G. A. M.; Gupta, V. K.; Makhlouf, A. S. H.; Shahryari-ghoshekandi, R.; Nadagouda, M. N.; Sillanpää, M.; Megiel, E. *J. Nanostruct. Chem.* **2017**, *7*, 1. **[Crossref]**

[3]   Kumar, S. V.; Babu, D. P. *Mater. Today: Proc.* **2024**. **[Crossref]**

[4]   Chen, Y. H.; Chen, Y. D. *J. Hazard. Mater.* **2011**, *185*, 168. **[Crossref]**

[5] Phoon, B. L.; Lai, C. W.; Juan, J. C.; Show, P. L.; Chen, W. H. Int. *J. Energy Res.* **2019**, *43*, 5151. **[Crossref]**

[6] Ay, E.; Aktaş, P. S. *React. Kinet., Mech. Catal.* **2023**, *136*, 1107. **[Crossref]**

[7] Ismail, W. N. W.; Syah, M. I. A. I.; Muhet, N. H. A.; Bakar, N. H. A.; Yusop, H. M.; Samah, N. A. *Civil Engineering Journal*. **2022**, *8*, 1787. **[Crossref]**

[8] Bitencourt, J. F. S.; Ventieri, A.; Gonçalves, K. A.; Pires, E. L.; Mittani, J. C.; Tatumi, S. H. *J. Non-Cryst. Solids.* **2010**, *356*, 2956. **[Crossref]**

[9] Oliveira, Y. L.; Costa, M. J. S.; Jucá, A. C. S.; Silva, L. K. R.; Longo, E.; Arul, N. S.; Cavalcante, L. S. *J. Mol. Struct.* **2020**, *1221*, 128774. **[Crossref]**

[10] Gonçalves, R. F.; Lima, A. R. F.; Godinho, M. J.; Moura, A. P.; Espinosa, J.; Longo, E.; Marques, A. P. A. *Ceram. Int.* **2015**, *41*, 12841. **[Crossref]**

[11] Subramanian, A.; Appukuttan, S. *ChemistrySelect.* **2019**, *4*, 7818. **[Crossref]**

[12] Zhu, Q. A.; Xu, J. G.; Xiang, S.; Chen, L. X.; Tan, Z. G. *Mater. Lett.* **2011**, *65*, 873. **[Crossref]**

[13] Rajkoomar, N.; Murugesan, A.; Prabu, S.; Gengan, R. M. *Phosphorus, Sulfur, and Silicon and the Related Elements* **2020**, *195*, 1031. **[Crossref]**

[14] Anand, D.; Ramachandran, K.; Sakthivel, P.; Silambarasan, M. *Ceram. Int.* **2024**, *50*, 33590. **[Crossref]**

[15] Deshmukh, V. V.; Ravikumar, C. R.; Kumar, M. R. A.; Ghotekar, S.; Kumar, A. N.; Jahagirdar, A. A.; Murthy, H. C. A. *Environ. Chem. Ecotoxicol.* **2021**, *3*, 241. **[Crossref]**

[16] Konstas, P. S.; Konstantinou, I.; Petrakis, D.; Albanis, T. *Catalysts* **2018**, *8*, 528. **[Crossref]**

[17] Soraes, M. D. A.; Alves, V. N.; *Rev. Processos Químicos* **2020**, *14*, 59. **[Crossref]**

[18] Chen, X.; Hossain, M. F.; Duan, C.; Lu, J.; Tsang, Y. F.; Islam, M. S.; Zhou, Y. *Chemosphere* **2022**, *307*, 135545. **[Crossref]**

[19] Huang, X.; Chen, T.; Zou, X.; Zhu, M.; Chen, D.; Pan, M. *Int. J. Environ. Res. Public Health* **2017**, *14*, 1145. **[Crossref]**

[20] Akpomie, K. G.; Conradie, J.; Adegoke, K. A.; Oyedotun, K. O.; Ighalo, J. O.; Amaku, J. F.; Olisah, C.; Adeola, A. O.; Iwuozor, K. O. *Appl. Water Sci.* **2023**, *13*, 20. **[Crossref]**

[21] Pereira, S. C.; Oliveira, J. A. N.; Siqueira, A. G.; Ferreira, M. M.; Alves, V. N. *Revista Processos Químicos* **2019**, *13*, 19. **[Crossref]**

[22] Sousa, D. G.; Oliveira, M. M.; Rangel, J. H. G.; Vasconcelos, J. S.; Longo, E. *Holos* **2017**, *5*, 55. **[Crossref]**

[23] Rosário, L. O.; Castro, M. A. M.; Tranquilin, R. L.; Teodoro, M. D.; Correa, M. A.; Motta, F. V.; Bomio, M. R. D. *J. Photochem. Photobiol., A* **2024**, *449*, 115402. **[Crossref]**

How to cite this article